Multijet and single diffraction dissociation Monte Carlo generator

J. C. Chen*
China Center of Advanced Science and Technology (World Laboratory), Beijing 100080, China

Q. Q. Zhu and A. X. Huo
Institute of High Energy Physics, Beijing 100039, China

(Received 2 July 1996; revised manuscript received 26 September 1996)

We have built a Monte Carlo generator for simulating propagation of cosmic ray particles in the atmosphere. The core of the generator is a p-air nuclear interaction model in which SD and NSD processes are included in the inelastic collisions. Based on QCD partonic theory, multiple minijet production is described in detail in the NSD process. A phase-space model is used for the SD process in our work. This generator reproduces cosmic ray experimental data well at very high energies. [S0556-2821(97)00805-9]

PACS number(s): 13.87.Ce, 13.85.Hd, 13.85.Tp, 96.40.De

I. INTRODUCTION

Before reaching a ground-based detector, a cosmic ray particle has typically undergone multiple interactions with air nuclei. Because the interactions are random processes, the interaction altitudes cannot be estimated reliably. In addition, the kinds of incident particles in ultrahigh energy (UHE) cosmic rays can only be estimated from the statistical distributions of low energy primary cosmic rays. All of these factors make for complications in the cosmic ray data analysis. Simulating the propagation of cosmic ray particles in the atmosphere and comparing the Monte Carlo (MC) samples with experimental data is an effective way to investigate the UHE nuclear interactions.

The basic frame of a Monte Carlo generator for the simulation of cosmic ray propagation in the atmosphere consists of the following parts.

(1) Incident particles energies are sampled from the energy spectrum of the primary cosmic rays. In this work, the primary UHE spectrum is a smooth extrapolation from the up-to-data direct observational data in the 10^{14} eV energy region [1].

(2) Cosmic ray particles interact with air nuclei and secondary particles are produced based on a multiple hadronic production model.

(3) The propagation processes of secondary particles are traced in air until they reach the ground-based detector or their energies are lower than the threshold energy of the detector.

The main part of a Monte Carlo generator is the proton-air (p-air) nuclear interaction model, and the key part of the p-air interaction model is a p-p interaction model. There are various p-p interaction models and they can be divided into two types according to their scaling behaviors in the so-called fragmentation region. The first type is the scaling violation model, such as the fire ball model, or the diffractive-nondiffractive (D-ND) model [2] which is based on the Zhou-Yang model; the other type of p-p interaction model is the scaling model. Recently, UA7 experimental data [25] have appeared to show as if hadronic interactions obey a scaling behavior at the fragmentation region in the accelerator energy range. When the UA1 group divided minimum bias events which were observed in the CERN Super Proton Synchrotron ($S\overline{p}pS$) into two kinds of events, jet events and no-jet events, they found that their characteristics are very different [3]. Both the multiple distribution and the transverse momentum distribution for jet events are wider than those distributions of no-jet events. The fraction of jet events in the hadronic interaction is greatly enhanced with an increase in energy. The increase of the inelastic cross section in the p-p interactions between the CERN Intersecting Storage Rings (ISR) and $S\overline{p}pS$ energy regions can be explained by the contribution of jet events. In recent years, some multiple particle production models with a hard partonic collision mechanism have been developed, such as the dual parton model (DPM) [4,5], Lund [6,7], ISAJET [8], and HIJING [9]. All of these models are used for describing hadronic interactions in detail at accelerator energies. However, such models cannot be simply scaled to the UHE range of cosmic rays. In typical cosmic ray experiments the detectors work in the very wide energy regions and do not distinguish the kinds of hadrons clearly. Although some Monte Carlo generators have been used for the simulation of cosmic ray propagation, they only include the production of a pair of large transverse momentum QCD jets [10–13]. In these models, because the inclusive jet cross section rises steeply following the incident particle energy increases, the cross section of a pair of jets would be larger than the total inelastic cross section at a high energy. In order to solve this problem, such models used a transverse momentum cut at momenta higher than 4 GeV/c.

In fact, according to investigations of semihard interactions in perturbative QCD (PQCD), the steep rise of the jet inclusive cross section means that the number of jets increases quickly in hadronic interactions at high energies. When selecting adaptive parameters, the cross section for multiple jet production will be less than total inelastic cross section and this is the idea behind the multiple minijet model. The UA1 group had claimed that they found multiple jets in the $S\overline{p}pS$ accelerator data. In this work, we present a

*Electronic address: chenjc@bepc5.ihep.ac.cn or chenjc@hpws5.ihep.ac.cn

new Monte Carlo generator in which the multiple minijet production is included in the nonsingle diffraction (NSD) process of nuclear interactions; soft hadrons are assumed to follow the Feynman scaling rule and the single diffraction (SD) process is described by a phase space model. We call this generator a multijet and single diffraction dissociation (MJSD) model. According to our simulation, the MJSD model can reproduce cosmic ray experimental data very well.

II. p-p COLLISION

Multiple minijet production can be described by PQCD theory with a partonic collision in the hadronic interaction. In the parton-parton collision, a pair of back-to-back jets is produced by two hard parton scattering events. The inclusive cross section of jet events can be written as

$$\frac{d\sigma_{\rm jet}}{dP_T d\theta}(A+B\rightarrow {\rm jet}+X) = \frac{1}{2}\frac{2\pi P_T^2}{E\sin^2\theta}0.3894\,\frac{K}{\pi}\sum_{a,b}\int_{x_a^{\rm min}}^{1.0}dx_a \times\frac{x_b^2}{x_2}f_a^A(x_a,Q^2)f_b^B(x_b,Q^2)\frac{d\hat{\sigma}}{d\hat{t}}, \quad (1)$$

where the partonic structure function $f_a^A(x_a,Q^2)$ describes the possibility of a parton with energy fraction x_a in the hadron A, and the Duke-Owens structure function set 1 [14] is used. The factor $K\approx 2$ is used to correct the lowest order PQCD rates for next to leading order effects. The transverse momentum P_T is expressed in GeV/c.

At a scale $P_0\sim 2$ GeV/c, partonic collisions are presumed to be independent [9] and the average number of minijets in the collision of a pair of nucleons is

$$N_{\rm jet}=T_N(b)\sigma_{\rm jet}, \quad (2)$$

where $T_N(b)$ is partonic overlap function of two nucleons at impact parameter b. According to the independent collision approximation, $N_{\rm jet}$ follows the Poisson distribution. With collision parameter b, the possibility of a number of multiple minijets, $N_{\rm jet}$, with a J pair is [9,15,16]

$$g_j(b)=\frac{[\sigma_{\rm jet}T_N(b)]^J}{J!}e^{-\sigma_{\rm jet}T_N(b)}. \quad (3)$$

The probability of $J=0$ is related to the nonperturbative cross section $\sigma_{\rm soft}$ by

$$g_0=[1-e^{-\sigma_{\rm soft}T_N(b)}]e^{-\sigma_{\rm jet}T_N(b)}. \quad (4)$$

The total inelastic cross section for a p-p collision is

$$\sigma_{\rm in}=\int_0^\infty db^2\sum_{J=0}^\infty g_j(b) = \int_0^\infty db^2[1-e^{-(\sigma_{\rm soft}+\sigma_{\rm jet})T_N(b)}]. \quad (5)$$

In the impact parameter representation, ignoring spin-dependent effects and assuming that the p-p scattering amplitude is purely imaging at high energy, we have eikonal expressions for the total cross section $\sigma_{\rm tot}$, the inelastic cross section $\sigma_{\rm in}$, and the elastic cross section $\sigma_{\rm el}$ [17–20]:

$$\sigma_{\rm el}=\pi\int_0^\infty db^2(1-e^{-\chi(b,s)})^2, \quad (6)$$

$$\sigma_{\rm in}=\pi\int_0^\infty db^2(1-e^{-2\chi(b,s)}), \quad (7)$$

$$\sigma_{\rm tot}=2\pi\int_0^\infty db^2(1-e^{-\chi(b,x)}). \quad (8)$$

By comparing formula (5) with (7), $\chi(b,s)$ can be expressed as

$$\chi(b,s)=\chi_s(b,s)+\chi_h(b,s)=\tfrac{1}{2}\sigma_{\rm soft}T_N(b,s)+\tfrac{1}{2}\sigma_{\rm jet}T_N(b,s). \quad (9)$$

We follow the assumption proposed in the HIJING model [9] that the energy-dependent partonic overlap function can be approximated by the Fourier transformation of a dipole form factor

$$T_N(b,s)=\frac{\chi_0(\xi)}{\sigma_{\rm soft}}, \quad (10)$$

with

$$\chi_s(b,s)=\tfrac{1}{2}\chi_0(\xi),$$

$$\chi_h(b,s)=\tfrac{1}{2}\frac{\sigma_{\rm jet}}{\sigma_{\rm soft}}\chi_0(\xi),$$

$$\chi_0(\xi)=\frac{\mu_0^2}{48}(\mu_0\xi)^3K_3(\mu_0\xi),$$

where χ_0 satisfies

$$\int_0^\infty \xi d\xi\chi_0(\xi)=1$$

and where $\xi=b/b_0$, $\mu_0=3.9$, $\pi b_0^2\equiv\sigma_{\rm soft}/2$, $\sigma_{\rm soft}=57$ mb, and the unit of b is fm. The total probability of J pairs of jets with momentum $P_T\geqslant P_0$ produced in an inelastic p-p collision is given by the integration of $g_0(b)$ and $g_J(b)$:

$$G_0=\frac{\pi}{\sigma_{\rm in}}\int_0^\infty db^2[1-e^{-2\chi_s(b,s)}]e^{-2\chi_h(b,s)}, \quad (11)$$

$$G_J=\frac{\pi}{\sigma_{\rm in}}\int_0^\infty db^2\frac{[2\chi_h(b,s)]^J}{J!}e^{-2\chi_h(b,s)} \quad (J\geqslant 1). \quad (12)$$

III. MULTIPLE NUMBER DISTRIBUTION OF MINIJETS IN THE NSD EVENTS

The UA4 and UA5 groups of CERN's S$\overline{pp}$S and the E710 group of Fermilab have observed SD and NSD phenomena in inelastic collisions. When cosmic rays propagate in the atmosphere, the particles produced in the SD process will be much more likely to reach the ground due to their

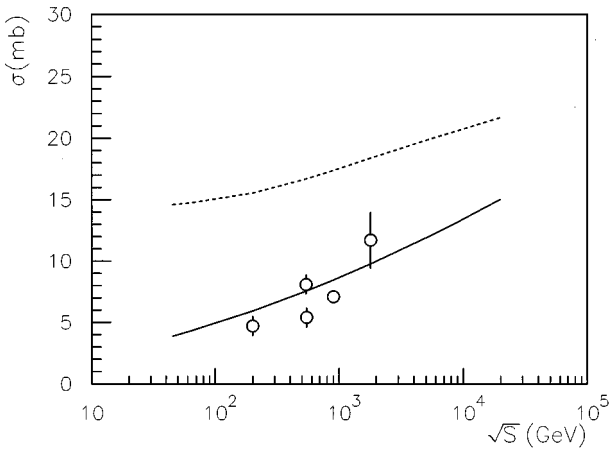

FIG. 1. SD cross section in the pp interaction. The dashed line is the $\sigma_{\rm SD}^{\rm up\ limit}$ by Eq. (16) and the solid line is the $\sigma_{\rm SD}$ calculated using formula (14). The circles are $\sigma_{\rm SD}^{\rm expt}$ from Refs. [21–24,26].

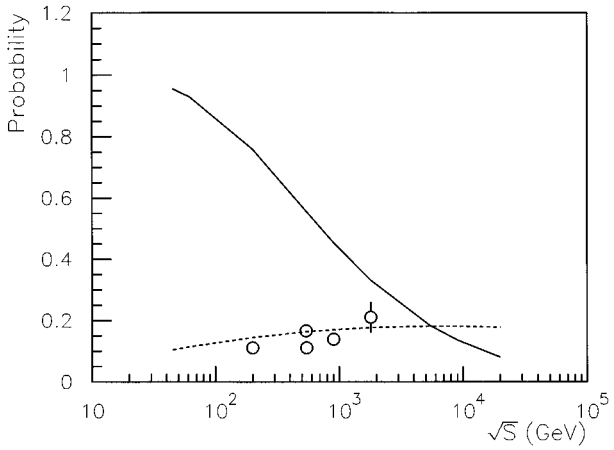

FIG. 2. $P_{\rm SD}$ and G_0 in inelastic processes. The solid line is G_0 calculated using Eq. (11) and the dashed line is $P_{\rm SD}$ defined by formula (15). Circles are experimental data of $P_{\rm SD}$ from Refs. [21–24,26].

smaller number of multiple production and less energy loss per event. The SD process plays an important role in cosmic ray propagation in the atmosphere, so that the SD contribution as well as jet production must be included in our Monte Carlo generator. The multiple number distribution of minijets in inelastic events can be explained by the eikonal formula; however, we still do not know the distribution in NSD process. According to accelerator experiments the inelastic cross section consists of the SD cross section and the NSD cross section, $\sigma_{\rm in}=\sigma_{\rm SD}+\sigma_{\rm NSD}$. The fraction of $\sigma_{\rm SD}$ in the $\sigma_{\rm in}$ is

$$P_{\rm SD}=\frac{\sigma_{\rm SD}}{\sigma_{\rm in}}. \tag{13}$$

We inferred this ratio by fitting accelerator experimental data [21–24,26] as

$$\sigma_{\rm SD}=0.5803+0.4903\ln\sqrt{s}+0.0981\ln^2\sqrt{s}, \tag{14}$$

$$P_{\rm SD}=\frac{\sigma_{\rm SD}}{\sigma_{\rm in}}=-0.0625+0.0561\ln\sqrt{s}-0.0032\ln^2\sqrt{s}, \tag{15}$$

where $\sqrt{s}$ is in GeV and the cross section is in mb. According to the UA4, UA5, and E710 experimental results, $\sigma_{\rm SD}$ and $P_{\rm SD}$ rise slowly following an energy increase and it is difficult to judge in which energy region they will decrease. Based on unitarity bound of the diffraction process, it can be inferred that the upper limit of the single diffraction cross section is [27]

$$\sigma_{\rm SD}^{\rm up\ limit}=\tfrac{1}{2}\sigma_{\rm tot}-\sigma_{\rm el}. \tag{16}$$

It can be seen from Fig. 1 that our formula of the SD cross section does not contradict the theory upper limit.

In order to include the SD cross section into the minijet model, it has been suggested that SD can be attributed to the softer parts of the scattering process [15]. However, in such a model the SD cross section will decrease quickly with increasing energy and this obviously contradicts the accelerator data. In addition the ratio of the SD cross section to the total inelastic cross section, $P_{\rm SD}=\sigma_{\rm SD}/\sigma_{\rm in}$, will increase the total value of G_0 (which describes the soft process in our model) if $\sigma_{\rm SD}$ does not decrease quickly when $\sqrt{s}$ excesses 5 TeV (as seen in Fig. 2). In other words, the probability of no-jet production in inelastic events, G_0, which is calculated from Eq. (11), cannot include the probability of single diffraction processes in the UHE region.

In order to include the SD process in the eikonal formula for inelastic collisions in a simple way, we suppose that the SD events were produced from particle edge collisions in our model. From the mathematical point of view, it is assumed that the SD cross section comes from the large impact parameter (high order wave function) contribution. Based on this assumption the eikonal formula for $\sigma_{\rm SD}$ and $\sigma_{\rm NSD}$ can be taken to be

$$\sigma_{\rm SD}=\pi\int_{b_{\rm SD}}^{\infty}db^2(1-e^{-2\chi(b,s)}), \tag{17}$$

$$\sigma_{\rm NSD}=\pi\int_{0}^{b_{\rm SD}}db^2(1-e^{-2\chi(b,s)}), \tag{18}$$

$$\sigma_{\rm in}=\sigma_{\rm SD}+\sigma_{\rm NSD}=\pi\int_{0}^{\infty}db^2(1-e^{-2\chi(b,s)}), \tag{19}$$

where the parameter $b_{\rm SD}$ can be inferred by fitting $\sigma_{\rm SD}$ and $\sigma_{\rm NSD}$ with experimental data in p-p collisions, that is,

$$b_{\rm SD}(s)=6.243-0.4364\ln\sqrt{s}+0.027\ 25\ln^2\sqrt{s}. \tag{20}$$

The unit of $\sqrt{s}$ is GeV, and the unit of b is fm. The results for $\sigma_{\rm SD}$ and $\sigma_{\rm NSD}$ by these parametrized formulas (17) and (18) are shown in Fig. 3, and there is no obvious contradiction with any experimental data up to the present time.

The probability of no-jet events in NSD events can be inferred from the eikonal formula given above as

$$G_0^{\rm NSD}=\frac{\pi}{\sigma_{\rm NSD}}\int_0^{b_{\rm SD}}db^2(1-e^{-2\chi_s(b,s)})e^{-2\chi_h(b,s)}. \tag{21}$$

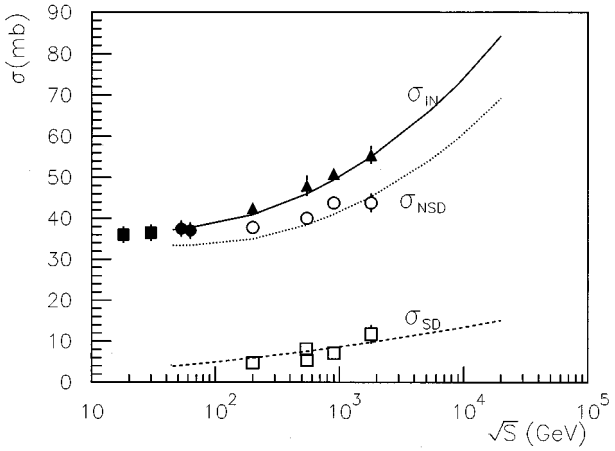

FIG. 3. Cross sections in the pp interaction. The solid line is $\sigma_{\text{inelastic}}$, the dotted line is σ_{NSD}, and the dashed line is σ_{SD} which are calculated using parametrized formulas (17)–(19). The symbols are experimental data from Refs. [21–24,26], where solid symbols are $\sigma_{\text{inelastic}}$, open circles are σ_{NSD}, and open squares are σ_{SD}.

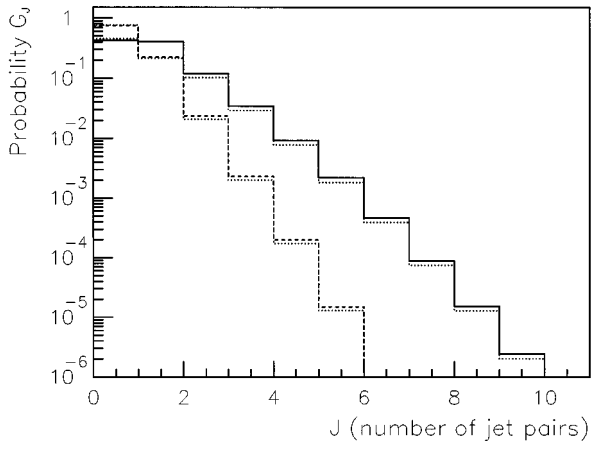

FIG. 4. Probability of jet number for NSD processes in the pp interaction (G_0 G_J). The solid line is for $\sqrt{s}=900$ GeV, the dashed line is for $\sqrt{s}=200$ GeV in the NSD process by formulas (21) and (22), and the dotted lines are for 900 and 200 GeV in the inelastic process by formulas (11) and (12).

The probability of J pair jet events in NSD is given by

$$G_J^{\text{NSD}}=\frac{\pi}{\sigma_{\text{NSD}}}\int_0^{b_{\text{SD}}} db^2\,\frac{[2\chi_h(b,s)]^J}{J!}e^{-2\chi_h(b,s)} \quad (J\geqslant 1), \tag{22}$$

where the G_j satisfy

$$G_0+\sum_{J=1}^{\infty} G_J=1. \tag{23}$$

The distribution of G_0^{NSD} and G_J^{NSD} are shown in Fig. 4.

IV. PARTON HADRONIZATION

According to QCD quarks and gluons cannot reach free states so that they can be detected only by their secondary hadrons produced in the partonic fragmentation. Following the assumption proposed in the SD-SH model [12], the partonic fragmentation functions used in our model are taken as

$$D_q(z)=z^{\alpha(s)}e^{-\beta(s)z} \tag{24}$$

for quarks and

$$D_g(z)=z^{dg}(1-z)D_q(z) \tag{25}$$

for gluons, where z is longitudinal momentum fraction,

$$z=\frac{2P_L}{\sqrt{s}}, \tag{26}$$

and the transverse momentum distribution is

$$f(P_T)=b^2P_Te^{-bP_T}, \tag{27}$$

where

$$\frac{1}{b}=\frac{\langle P_T\rangle}{2}=0.227+0.0462\ln P_L+0.0081\ln^2P_L. \tag{28}$$

The seagull effect has been included here. In order to conserve energy after sampling z_n from the above distribution, the real longitudinal momentum fraction is taken to be

$$z_n'=z_n\left(1-\sum_{i=1}^{n-1} z_i'\right). \tag{29}$$

The parameters of this fragmentation function are inferred by fitting e^+e^- collider data.

Our Monte Carlo results for jet fragmentation are consistent with e^+e^- experimental data for (a) the momentum fraction of charged particle distribution X_p, (b) the transverse momentum distribution P_T, (c) the pseudorapidity distribution η, and (d) the mean charged multiplicity distribution. The comparative results are shown in Figs. 5(a)–5(d).

V. FEYNMAN SCALING SOFT INTERACTION

In NSD events, both the G_0 (no jet) particle's fragmentation and the spectator particle's fragmentation are soft hadronic interactions. The soft interaction cannot be calculated by PQCD, so that it becomes necessary to apply a phenomenological model to describe the soft process. In the MJSD generator, the soft hadrons are assumed to follow the Feynman scaling distribution

$$f(x_f)=\frac{(1-x_f)^5}{x_f}, \tag{30}$$

$$x_f=\frac{2P_L}{\sqrt{s}}, \tag{31}$$

with the transverse momentum following a distribution given by

$$f(P_T)=b^2P_Te^{-bP_T}, \tag{32}$$

$$\frac{1}{b}=\frac{\langle P_T\rangle}{2}=0.105+0.063\ln P_L+0.0084\ln^2P_L. \tag{33}$$

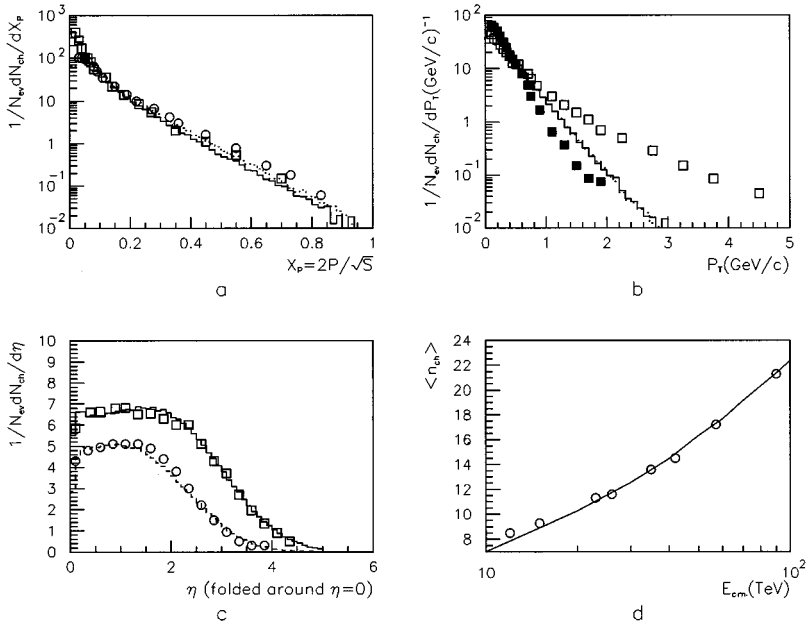

FIG. 5. The comparative results between the e^+e^- collider data and the jet fragmentation by the MJSD model. The lines are results of the MJSD model and symbols are experimental data from Refs. [28–32]. In (a) the solid line and squares are for $\sqrt{s}=91$ GeV, and the dotted line and circles are for $\sqrt{s}=22$ GeV. In (b) the solid line and the solid square are for P_T^{out} and the dotted line and empty square are for P_T^{in} at $\sqrt{s}=91$ GeV. In (c) the solid line and square are for $\sqrt{s}=91$ GeV and the dashed line and circle are for $\sqrt{s}=29$ GeV.

Because this generator is used for UHE cosmic ray data and a typical detector in such experiments cannot distinguish hadron types in most cases, the following assumptions are made in this model: Secondary particles are 90% pions, 10% kaons, and a few η's, with 60% of all secondaries charged and 40% neutral. Inelastic efficiency is assumed to be a uniform distribution from 0 to 96%. The species of the leading particle is assumed the same as the incident particle. Multiplicity numbers presumably obey a KNO distribution and the mean multiplicity number rises with energy as ln(s).

VI. FRAMEWORK OF THE NSD GENERATOR OF *p-p* COLLISION

In the inelastic of *p-p* collisions, the framework of a NSD events generator is taken as follows.

(1) N_{jet}, number of jet produced in NSD, is sampled from the G_0 and G_J distributions.

(2) Characteristics of jets are sampled in the following way. (a) transverse momentum of the C jet (forward jet) is sampled from

$$f(P_T)=\frac{\int_{P_T}^{\infty}dP_T\int_0^{\pi}(d\sigma_{\text{jet}}/dP_T d\theta)d\theta}{\int_{P_0}^{\infty}dP_T\int_0^{\pi}(d\sigma_{\text{jet}}/dP_T d\theta)d\theta}. \tag{34}$$

(b) The angular distribution of the C jet is given by

$$f(\theta|P_T)=\frac{\int_{\theta}^{\pi}(d\sigma_{\text{jet}}/dP_T d\theta)d\theta}{\int_0^{\pi}(d\sigma_{\text{jet}}/dP_T d\theta)d\theta}. \tag{35}$$

(c) The fraction of gluon jets is described by the distribution

$$f_g(P_T)=\frac{\sigma_g(P_T)}{\sigma_{\text{jet}}(P_T)}. \tag{36}$$

(d) The momentum fraction of the C jet is

$$x_C=\frac{P_T}{\sin\theta_C\sqrt{S}/2}. \tag{37}$$

(e) The transverse momentum of a backward jet (D jet) is the same as the C jet's P_T. (f) The fraction of the D-jet momentum x_D is sampled from the $\overline{x_D}$ jet distribution. (g) The emission angle of the D jet is taken as

$$\sin\theta_D=\frac{P_T}{X_d\sqrt{S}/2}. \tag{38}$$

(3) No jet events (energy fraction G_0) and spectator particle fragmentations [their energy fractions are $(1-\Sigma x_C)\sqrt{S}/2$ and $(1-\Sigma X_D)\sqrt{S}/2$] are taken to be soft hadronic interactions.

In a comparison of our Monte Carlo results with NSD data from *p-p* collisions in accelerator experiments, Figs. 6(a)–6(f) show that the MJSD generator can reproduce most important experimental features, such as (a) the pseudorapidity distribution, (b) P_T distribution, (c) charged Koba-Nielsen-Olesen (KNO) distribution, (d) jet event charged KNO distribution, (e) mean charge multiplicity distribution, and (f) $P_T-dn/d\eta$ distribution.

VII. SD PROCESS

Diffraction dissociation is a process of coherent hadron fragmentation. In diffraction dissociation a secondary particle cluster can carry large invariant mass, and its inner quantum numbers are the same as the incident hadron. Its main characteristic is an obvious rising forward differential cross section [40–42]. There is no mature theoretical model for the SD process up to now. A workable approach to the problem would be to study the SD process in momentum phase space using a phenomenological model.

In this paper a phenomenological model of the SD process, which was developed in our laboratory [43], is used in our MJSD generator. In this model, SD is taken to be the

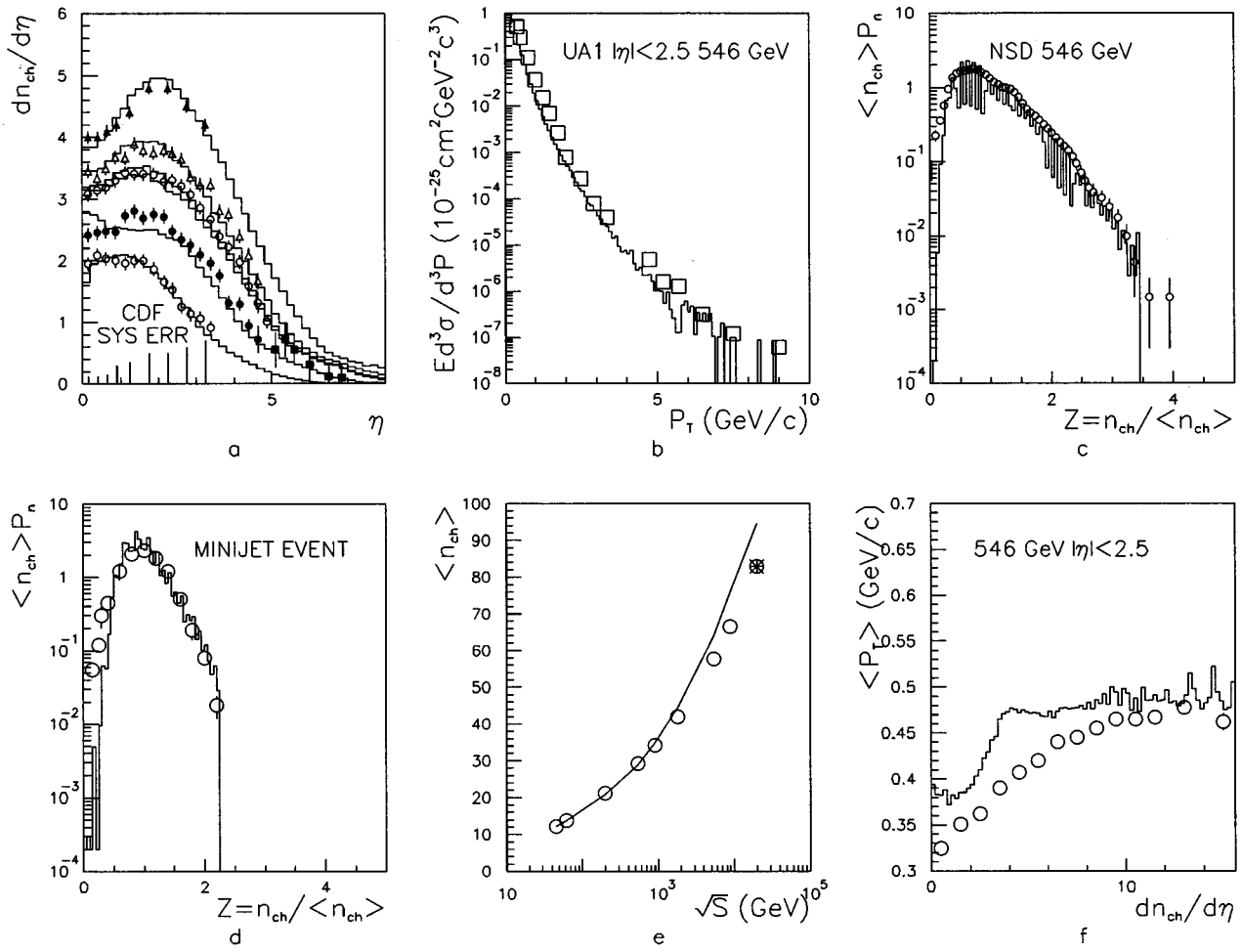

FIG. 6. The comparative results between the NSD data of p-p collisions and Monte Carlo samples of the MJSD model. The lines are results of the MJSD model and symbols are experimental data. (a) Energy regions are 53, 200, 546, 630, 900, and 1800 GeV and data are from Refs. [33–36,25]. (b) Squares are UA1 data [37]. (c) KNO distribution of NSD at 546 GeV; circles are from Ref. [24]. (d) KNO distribution of NSD jet events selected by UA1 criterion [1]; circles are data from Ref. [38]. (e) Circles are by UA5 formula [24]: $\overline{N_{\rm ch}}=-7.5+7.6s^{0.124}$. (f) Circles are data from Ref. [39].

decay process of the excited incident hadron. The longitudinal phase space technique is used [44,45], and SD experimental data are reproduced very well by this model. Its main characteristics are the following.

(1) The distribution of the invariant mass of the SD system is given by

$$\frac{dN}{d(M^2/S)} \propto \frac{1}{M^2/S}$$

$$(1.414\ \text{GeV} < M < 0.22\sqrt{s}),$$

because there are many spikes in the experimental data when $M^2 < 2$ GeV, so that a uniform mean distribution is assumed.

(2) The SD system is deexcited by emitting mesons uniformly in phase space.

(3) The transverse momentum of the secondary particles follows a distribution given by

$$f(P_T) \propto P_T e^{-P_T/b}, \tag{39}$$

where $b=\langle P_T\rangle/2=240$ MeV/c.

(4) Among the secondary particles, 10% are presumed to be kaons with 90% being pions. The number of charged kaons is taken to be the same as that of uncharged kaons. π^0, π^+, and π^- are assumed to be produced in equal numbers as well.

(5) Energy and momentum are conserved in the model.

VIII. p-AIR COLLISION

In the UHE region, the p-air nuclear interaction can be treated as the interaction of a proton with all nucleons of an air nucleus [15]. According to the independent nucleon model, the parton structure function in the air nucleus can be taken as $f_{a/\text{air}}(x)=Af_{a/N}(x)$, where $f_{a/N}(x)$ is the parton structure function in a free nucleon and A is the air nucleus mass number. In other words, the hard collisions of patrons are treated as point collisions so that $\sigma_{\text{jet}}^{p\text{-air}}=A\sigma_{\text{jet}}^{p\text{-}N}$. However, there are screen effects in the p-air soft interaction because its cross section is large. In the MJSD generator, for the p-air interaction the soft cross section $\sigma_{\text{soft}}^{p\text{-air}}$ is taken to be about $A^{2/3}\sigma_{\text{soft}}^{p\text{-N}}$ In the p-air collision, $\sigma_{\text{soft}}^{p\text{-air}}$ is taken to be 330 mb.

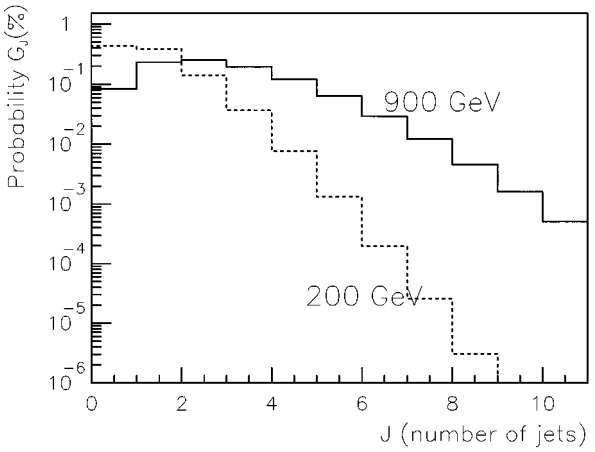

FIG. 7. G_0, G_j distributions of NSD process for the p-air interaction.

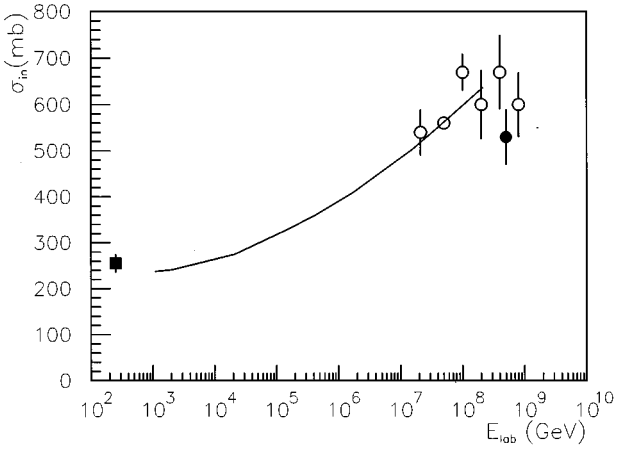

FIG. 8. The absorptive cross section for the p-air interaction. The line is by the MJSD model. The solid square is data from Fermilab [52], solid circle is data from Fly's Eye [53], and open circles are data from Akeno [54].

In fact, according to heavy ion collider experimental data, the hard interactions of patrons cannot be treated simply as point collisions, even at high energies. In collider experimental results the ratio

$$R_A(x)=\frac{1}{A}\frac{f_{a/A}(x)}{\frac{1}{2}f_{a/D}(x)}\neq 1. \tag{40}$$

$R_A(x)$ obviously decreases both in regions of $x\leqslant 0.1$ (the parton shadowing effect) and $0.3\leqslant x\leqslant 0.7$ [the European Muon Collaboration (EMC) effect].

Among parton models there are several explanations for parton shadowing. Some attribute it to coherent interactions between the backward scattered parton and the parton in the nucleon, while others attribute it to gluon recombination in the high density collision state [46–48]. In an effort to explain the EMC effect, some have proposed that it is due to the changes of binding characteristics of nucleons [49,50].

Following a proposed parametrization [47,48,51,9], target-nucleus effects are described with $R_A(x,r)$ (where r is the distance from the parton to the nuclear center) given by

$$\begin{aligned}R_A(x,r)&=\frac{f_{a/A}(x)}{Af_{a/N}(x)}\\&=1+1.19\ln^{1/6}A[x^3-1.5(X_0+X_L)x^2+3X_0X_Lx]\\&\quad-\left[\alpha_A(r)-\frac{1.08(A^{1/3}-1)}{\ln(A+1)}\sqrt{x}\right]e^{-x^2/X_0^2},\end{aligned} \tag{41}$$

where $X_0=0.1$, $X_L=0.7$, and

$$\alpha_A(r)=0.1(A^{1/3}-1)\frac{4}{3}\sqrt{1-\frac{r^2}{R_0^2}}. \tag{42}$$

R_0 is the radius of the nucleus. If a uniform distribution of nucleons is assumed in the nucleus, the nuclear overlap function for a uniform sphere is

$$T_A(r)=\frac{3A}{2\pi R_A^2}\sqrt{1-\frac{r^2}{R^2}},$$

$$\frac{1}{A}\int_0^{R_0^2}\pi T_A(r)dr^2=1. \tag{43}$$

We carry out the integration over r:

$$\alpha_A=\frac{1}{A}\int_0^{R_0^2}\pi T_A(r)\alpha_A(r)dr^2=0.1(A^{1/3}-1), \tag{44}$$

$$\begin{aligned}R_A(x)&=\frac{1}{A}\int_0^{R_0^2}\pi T_A(r)R_A(x,r)dr^2\\&=1+1.19\ln^{1/6}A[x^3-1.5(X_0+X_L)x^2+3X_0X_Lx]\\&\quad-\left[\alpha_A-\frac{1.08(A^{1/3}-1)}{\ln(A+1)}\sqrt{x}\right]e^{-x^2/X_0^2},\end{aligned} \tag{45}$$

$$f_{a/A}(x)=Af_{a/N}(x)R_A(x). \tag{46}$$

TABLE I. Composition of primary cosmic rays in this work.

E (TeV)	$J(\mathrm{m}^{-2}\ \mathrm{sec}^{-1}\ \mathrm{sr}^{-1})$	p	He	CNO[a]	Ne-S[b]	Sub-Fe[c]
30	3.51×10^{-4}	0.345	0.300	0.122	0.069	0.164
110	3.66×10^{-5}	0.331	0.332	0.111	0.056	0.169
500	2.62×10^{-6}	0.316	0.374	0.098	0.042	0.170
1000	7.85×10^{-7}	0.308	0.395	0.092	0.037	0.169

[a] $Z=6$–8.
[b] $Z=10$–16.
[c] $Z\geqslant 17$.

TABLE II. Mean features of families.

ΣE_i[a] (TeV)	$\langle \Sigma E_i \rangle$[b] (TeV)		$\langle E_i \rangle$[c] (TeV)		$\langle N \rangle$[d]	
	Expt.	MC	Expt.	MC	Expt.	MC
20–50	37 ± 7	34 ± 6	7.8 ± 1.6	7.2 ± 1.4	4.7 ± 0.8	4.7 ± 0.7
50–100	67 ± 14	68 ± 13	9.3 ± 1.9	9.7 ± 1.9	7.2 ± 0.4	7.1 ± 0.1
100–200	126 ± 26	134 ± 27	11.3 ± 2.3	11.1 ± 2.2	11.2 ± 0.9	12.1 ± 0.1

[a]E is the observed energy of a particle and the ΣE_i is the observed energy of a family.
[b]Mean energy of families.
[c]Mean energy of particles.
[d]Mean number of particles in a family.

The p-air cross section can now be obtained with $f_{b/\text{air}}(x_b,Q^2)=A_{\text{air}}f_{b/N}(x_b,Q^2)R_A(x)$ [instead of $f_b^B(x_b,Q^2)$] in Eq. (1). For p-air interactions, all distributions of jets can be calculated by analogy with those formulas for p-p interactions. So replacing $\sigma^{p\text{-}p}$ with $\sigma^{p\text{-air}}$, the P_T distribution, and θ distribution of jets as well as the G_0 and G_J distributions of jets can be obtained. The shapes of p-air G_0 and G_J distributions are shown in Fig. 7. The fraction of σ_{SD} in σ_{in} is assumed to be the same as for p-p interactions. The integration limit used to obtain $\sigma_{\text{SD}}^{p\text{-air}}$ and $\sigma_{\text{NSD}}^{p\text{-air}}$ in formulas (17) and (18) is parametrized as

$$b_{\text{SD}}^{p\text{-air}}(s)=5.038+0.0643\ln\sqrt{s}+0.0058\ln^2\sqrt{s}. \quad (47)$$

From Fig. 8 we can see that although p-air collisions are treated simply in the MJSD model, the absorptive cross section for p-$p$air interaction experimental data can be reproduced by MC samples at UHE region very well.

Up to now, we have presented all the details of the MJSD model, and we have reported that this model can reproduce a lot of e^+e^- and proton-antiproton accelerator experimental results, as well as the absorptive cross section for the p-air interaction at UHE. In the following section we will apply the MJSD model to illustrate several published experimental data observed in a large scale Mountain Emulsion Chamber (MEC) cosmic ray experiment.

IX. CALCULATIONS FOR THE MEC COSMIC RAY EXPERIMENT

Large scale MEC experiments usually consist of alternatively placed films and metal plates. They concern features of the UHE hadronic interaction in the fragmentation region mainly [11]. ''Family'' events are observed in the MEC experiment, which consist of some parallel incident particles originated by a UHE primary cosmic ray in the atmosphere. Family events are divided into two classes, i.e., ''γ family'' and ''hadron family.'' The former is composed of only γ rays (abbreviation of electromagnetic components) and the latter is composed of both γ rays and hadrons.

The intensity of γ families is known to depend sensitively on UHE nuclear interaction features and composition of primary cosmic rays. In Sec. I, we have described the basic frame of the Monte Carlo generator for the simulation of cosmic ray propagation in atmosphere. In our simulation, the UHE primary cosmic ray spectrum (see Table I) is a smooth extrapolation from the direct observational data in the about 10^{14} eV energy region in Ref. [2]. It should be noticed that this primary spectrum is compatible with JACEE recent experimental results too [56]. Based on this primary cosmic spectrum, we apply the MJSD model to simulate MEC family phenomena. The comparisons of some average features of families between experimental data and MC samples in the energy region from 20 TeV to 200 TeV are shown in the Table II. According to the Monte Carlo simulation, more than 90% of these families were produced by primary cosmic ray particles with energy in the region from 3×10^{13} eV to 10^{15} eV. The intensity of experimental families and MC samples are compared in Fig. 9 and it can be seen that the intensity of MC samples is consistent with both sets of experimental data in Refs. [11,55].

The attenuation length of families in the atmosphere is another important quantity of the family phenomena related to p-air interaction features. The family events attenuate in accordance with the rule of $\exp(-x/\lambda)$ in the atmosphere, where x is the height of observation ($x=520$ g/cm^2 at Mt. Kanbala, China) and λ is the attenuation length. The attenuation length can be inferred from the zenith angle distribution of families, and it is (98 ± 8) g/cm^2, obtained with our MC families the energies of which are greater than 20 TeV. It can be compared to the length of (106 ± 22) g/cm^2, obtained with experimental data at the same family energy region in Ref. [55], and the length of (110 ± 10) g/cm^2, ob-

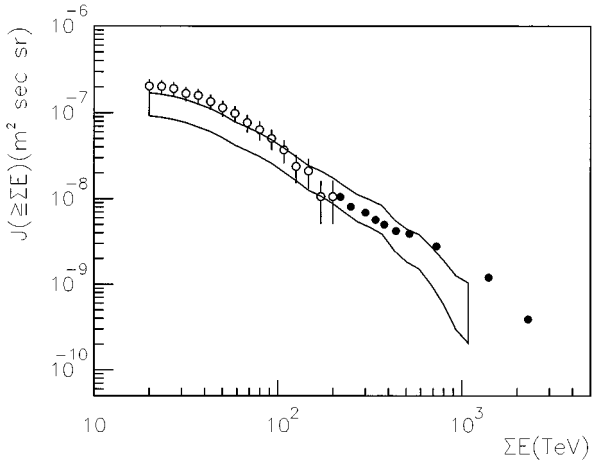

FIG. 9. γ family intensity at Mt. Kanbala altitude (Tibet of China, 5500 m above sea level, atmospheric depth 520 g/cm^2). Solid circles are data from Ref. [11] and open circles are data from Ref. [55]. The line is given by the MJSD model in which the errors of primary UHE cosmic ray spectra have been included.

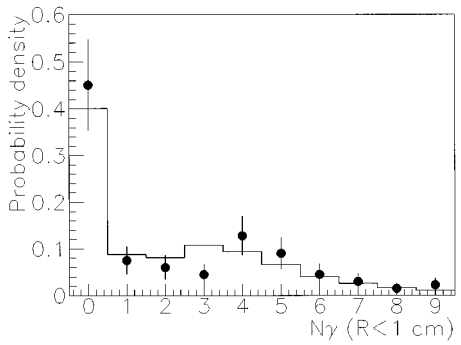

FIG. 10. Multiplicity distribution of particles near the center of families ($R<1$ cm). Solid circles are data from Ref. [55], and the line is calculated by the MJSD model.

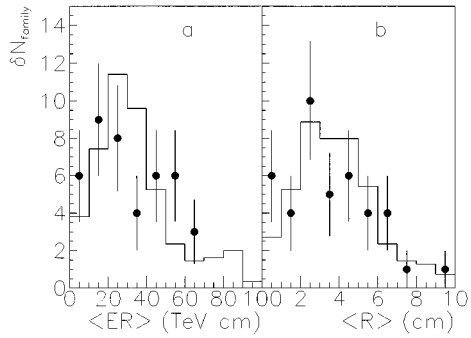

FIG. 11. (a) The differential distribution of lateral spread $\langle ER\rangle$ for hadron families. (b) The differential distribution of lateral spread $\langle R\rangle$ for hadron families, where the symbols ● stand for the distribution of data from Ref. [55] and lines are distributions of MC samples produced by the MJSD model.

tained in experiment [11] with families the energies of which are higher than 100 TeV.

The multiplicity distribution of particles near the center of the family relates to the p-air nuclear interaction features in the fragmentation region. The comparison of our MC samples and experimental data, in which the family energies are greater than 20 TeV, is shown in Fig. 10. It can be seen from the figure that the MC result is in agreement with the data very well.

It is well known that lateral spreads of families relate sensitively to the transverse momentum of secondary particles in the hadronic interactions and to the electrons emitting angles in the electromagnetic cascade, so that the lateral spread of secondaries in MEC data can provide us some information on the hadronic interaction model. The differential distributions of average lateral spreads $\langle ER\rangle$ and $\langle R\rangle$ for hadron families, the energies of which are greater than 20 TeV, are shown in Figs. 11(a) and 11(b), where the E is the observed energy of a particle and the R is the distance from the particle to the center of family, $\langle ER\rangle$ being the average value of $E\times R$. We can see from Fig. 11 that MC samples are compatible with the data in the statistical error.

It can be seen from Figs. 9, 10, and 11 and Table II that our MC samples and experimental data can reach agreement well. This means that the hadronic interaction parameters are reasonable in our MJSD model. Further results applying the MJSD model to investigate the MEC data in detail will be reported elsewhere.

X. REMARKS

SD and NSD processes have been included into the minijet model in the MJSD Monte Carlo generator. SD and NSD cross sections are consistent with all of the experimental data and do not contradict with the theory up to the limit in the UHE region. The major phenomenological features of accelerator-based experimental results are reproduced well by the MJSD model. We have applied the MJSD model to simulate the cosmic ray propagation in the atmosphere, and MC results accord with the family phenomena observed in the MEC cosmic ray experiment.

The present model is most suited to very high energies where semihard parton-parton interactions are dominant. In the UHE region, there are many unknown factors in the cosmic ray experiment, so that we obtain some information on hadronic interaction features usually by comparing the experimental phenomena to the MC samples. The MJSD model will provide a useful tool in the research of cosmic rays in which SD plays an important role in the process of cosmic ray propagation in the atmosphere.

ACKNOWLEDGMENTS

The authors would like to express their appreciation to Dr. X. N. Wang, Dr. Z. Cao, Professor L. K. Ding, Dr. J. R. Ren, Dr. S. L. Lu, and Dr. W. Q. Zhao for helpful discussions and to Peter Prymmer, David Smith, L. X. Cheng, and L. Ma for their very careful modifying of our manuscript.

[1] M. Ichimura *et al.*, Phys. Rev. D **48**, 1949 (1993).
[2] L. K. Ding, in Proceedings of the 5th International Symposium on VHE Cosmic Ray Interaction, Poland, 1988 (unpublished), p. 117.
[3] UA1 Collaboration, G. Arnison *et al.*, Phys. Lett. **132B**, 214 (1983).
[4] A. Capella *et al.*, Z. Phys. C **3**, 329 (1980).
[5] J. Ranft, Phys. Rev. D **37**, 1842 (1988).
[6] B. Andersson *et al.*, Nucl. Phys. **B281**, 289 (1987).
[7] B. Nilsson-Almgvist *et al.*, Comput. Phys. Commun. **43**, 387 (1987).
[8] F. E. Paige and S. D. Protopopescu, in *Physics of the Superconducting Super Collider, Snowmass, 1986*, Proceedings of the Summer Study, Snowmass, Colorado, edited by R. Donaldson and J. Marks (Division of Particles Fields of the APS, New York, 1987), p. 320.
[9] X. N. Wang and Miklos Gyulassy, Phys. Rev. D **44**, 3501 (1991).
[10] T. K. Gaisser and F. Halzen, Phys. Rev. Lett. **54**, 1754 (1985).
[11] J. R. Ren *et al.*, Phys. Rev. D **38**, 1404 (1988).
[12] Q. Q. Zhu *et al.*, J. Phys. G **16**, 295 (1990).
[13] Z. Cao *et al.*, Phys. Rev. Lett. **72**, 1794 (1994).

[14] D. W. Duke and J. F. Owens, Phys. Rev. D **30**, 49 (1984).
[15] L. Durand and H. Pi, Phys. Rev. D **38**, 78 (1988).
[16] T. K. Gaisser and T. Stanev, Phys. Lett. B **219**, 375 (1989).
[17] T. T. W and C. N. Yang, Phys. Rev. **137B**, 708 (1965).
[18] N. Byers and C. N. Yang, Phys. Rev. **142B**, 976 (1960).
[19] T. T. Chou and C. N. Yang, Phys. Rev. **170**, B1591 (1968).
[20] L. Durand and R. Lipes, Phys. Rev. Lett. **20**, 637 (1968).
[21] M. G. Albrow *et al.*, Nucl. Phys. **B108**, 1 (1976).
[22] D. S. Agres *et al.*, Phys. Rev. Lett. **37**, 1724 (1976).
[23] UA4 Collaboration, D. Bernard *et al.*, Phys. Lett. B **198**, 583 (1987).
[24] UA5 Collaboration, Phys. Rep. **154**, 247 (1987).
[25] UA7 Collaboration, in *Proceedings of the 21st International Cosmic Ray Conference*, Adelaide, Australia, 1989, edited by R. J. Protheroe (Graphic Services, Northfield, South Australia, 1990), Vol. 1, p. 29.
[26] E710 Collaboration, Phys. Lett. B **243**, 158 (1990).
[27] U. P. Sukhatme, Nucl. Phys. **B108**, 317 (1976).
[28] ALEPH Collaboration, D. Decamp *et al.*, Phys. Lett. B **234**, 209 (1990).
[29] TASSO Collaboration, M. Althoff *et al.*, Z. Phys. C **22**, 307 (1984).
[30] Mark II Collaboration, A. Pettersen *et al.*, Phys. Rev. D **37**, l (1988).
[31] TASSO Collaboration, W. Braunschwerg *et al.*, Z. Phys. C **45**, 193 (1989).
[32] MAY Collaboration, Y. K. Li *et al.*, Phys. Rev. D **41**, 2675 (1990).
[33] G. J. Alner *et al.*, Z. Phys. C **33**, 1 (1986).
[34] K. Alpgard *et al.*, Phys. Lett. **112B**, 193 (1982).
[35] F. Abe *et al.*, Phys. Rev. D **41**, 2330 (1990).
[36] CDF Collaboration, F. Abe *et al.*, Phys. Rev. Lett. **61**, 1819 (1988).
[37] UA1 Collaboration, G. Arnison *et al.*, Phys. Lett. **118B**, 167 (1982).
[38] J. G. Rushbrook, Report No. CERN-EP/85-178, 1985 (unpublished).
[39] G. Arnison, Phys. Lett. **118B**, 167 (1982).
[40] M. L. Good and W. D. Walker, Phys. Rev. **120**, 1857 (1960).
[41] K. Goulianos *et al.*, Phys. Rep. **101**, 169 (1983).
[42] R. L. Cool *et al.*, Phys. Rev. Lett. **48**, 145 (1982).
[43] Q. Q. Zhu *et al.*, J. Phys. G **20**, 1383 (1994).
[44] UA4 Collaboration, D. Bernard *et al.*, Phys. Lett. **166B**, 459 (1986).
[45] UA4 Collaboration, D. Bernard *et al.*, Phys. Lett. B **186**, 227 (1987).
[46] S. J. Brodsky and H. J. Lu, Phys. Rev. Lett. **64**, 1342 (1990).
[47] A. H. Mueller and J. Qiu, Nucl. Phys. **B268**, 427 (1986).
[48] J. Qiu, Nucl. Phys. **B291**, 746 (1987).
[49] R. L. Jaffe, Phys. Rev. Lett. **50**, 228 (1983).
[50] C. F. Carlson *et al.*, Phys. Rev. Lett. **51**, 281 (1983).
[51] L. L. Frankfurt and M. I. Strikman, Phys. Rep. **160**, 235 (1986).
[52] A. Carroll *et al.*, Phys. Lett. **80B**, 310 (1979).
[53] R. M. Baltrusaitis *et al.*, Phys. Rev. Lett. **52**, 1380 (1984); R. M. Baltrusaitis *et al.*, in Proceedings of the 19th ICRC, 1985 (unpublished), Vol. 6, p. 5.
[54] T. Hara *et al.*, Phys. Rev. Lett. **50**, 2058 (1983).
[55] J. C. Chen *et al.*, *High Energy Physics and Nuclear Physics* (Allerton, New York, 1995), Vol. 19, p. 233.
[56] JACEE Collaboration, in *Cosmic Ray Conference*, Proceedings of the 23rd International Conference, Calgary, Canada, 1993, edited by R. Hicks *et al.* (World Scientific, Singapore, 1994), Vol. 2, p. 21.